

Effect of ball-milling on the thermal properties of MgH₂/AlCrNiZrVNb materials for hydrogen storage

Lindokuhle Ntanzil^{1*}, Patricia Popoola¹, Olawale Popoola¹, Modupeola Dada¹

¹Department of Chemical, Metallurgical and Materials Engineering, Tshwane University of Technology, Pretoria, South Africa

Abstract. The preliminary study examined how ball milling influenced the thermal behavior of MgH₂/AlCrNiZrVNb materials to improve their energy storage potential. Both HEA and MgH₂ crystalline structures were observed, confirming that the material integrity was maintained during ball milling. The unmilled sample displayed highly crystalline structures with sharp, well-defined peaks, whereas the ball-milled samples showed broader peaks. This broadening indicates increased lattice strain, decreased crystallite size, and grain refinement resulting from ball milling, which can improve hydrogen storage kinetics. These findings highlight the potential of using ball milling to synthesize MgH₂ with HEA catalysts, advancing hydrogen storage technology for energy systems.

*Corresponding author: lindokuntanzi9@gmail.com

1 Introduction

Hydrogen has garnered significant attention as a clean energy carrier, particularly amid global efforts to reduce carbon emissions and divest from fossil fuels (Rasul et al., 2022). Advances in technologies such as electrolysis, fuel cells, and hydrogen storage have propelled this research, making hydrogen a key component of future clean energy systems (Usman, 2022). Molecular hydrogen (H₂) is highly diffusive, which impacts its storage and handling (Zhang et al. 2023). Due to its high reactivity, hydrogen can form various compounds, including water (H₂O) and metal hydrides (Younas et al. 2022). Despite having a high gravimetric energy density, hydrogen's low volumetric density makes it difficult to compress and liquefy; however, it remains a strong energy carrier (Rasul et al., 2022). Magnesium hydride (MgH₂) is a promising hydrogen storage material due to its high weight and volume hydrogen capacity, light weight, affordability, and availability (Yang et al., 2023). However, it faces challenges with poor kinetics and thermodynamics, necessitating catalyst enhancements (Hong et al. 2024). High-entropy alloys (HEAs) show potential catalytic activity because of their ability for atomic-scale customization and microstructural stability, which can improve the cycling performance of MgH₂ (Yu et al. 2022). HEAs are alloys composed of five or more principal elements, each with a concentration of 5 to 35 wt. % (Nene et al. 2024). Their unique properties including high strength, hardness, wear resistance, thermal stability, and corrosion resistance, enable various applications

(Tokarewicz et al. 2021). Higher configurational entropy reduces the Gibbs free energy of solid solution phases in HEAs, making their formation easier at high temperatures and decreasing phase diversity due to increased mutual solubility among elements (Zhang et al. 2024). Thermodynamic equilibrium helps determine phase stability in HEAs by comparing Gibbs free energies of potential phases to identify the most stable (Yang et al. 2025). HEAs also exhibit slower phase transformations and diffusion kinetics compared to conventional alloys. Lattice distortion caused by atoms of different sizes induces higher strain energy, which increases the free energy of the HEA lattice (Kumar, 2024). Most HEAs maintain good strength and hardness at high temperatures due to their resistance to thermal softening and their fabrication process (Tung et al. 2007). The fabrication method, particularly ball milling, is critical for optimizing HEA catalysts. Ball milling is a high-energy mechanical synthesis that induces microstructural changes necessary for catalysis (AlZoubi et al. 2023). It can form nanocrystalline structures that prevent catalyst degradation during repeated hydrogen absorption and desorption cycles. Ball milling enables control over structural features, allowing HEAs to effectively enhance the kinetics and cycling stability of MgH_2 (Yu et al., 2022). Therefore, this research aims to investigate the impact of ball milling on the thermal properties of HEA catalysts in MgH_2 for hydrogen energy storage.

2 Methodology and results

2.1 Materials selection

The Al, Cr, Ni, Zr, V and Nb HEA elemental powders of 99.5 % purity were weighed on an electronic weighing balance at 20% each and pre-mixed together. The powders with a particle size range of 45 to 150 μm were mixed using a tubular mixer for 8 hours at a speed of 49 rpm in a dry environment to homogenize the AlCrNiZrVNb high-entropy alloy powder mixture without agglomeration.

2.1.1 High energy ball milling

Planetary ball milling is a mechanical alloying process used in the manufacturing of engineering materials. The media are exposed to high energy with twenty times gravity centrifugal forces. The media and the powders in the vial, when milled, roll in the inner wall and become accelerated at high speed. Operating in a glove box is simple. In the current work, a Retsch 400M stainless steel planetary ball mill was utilized to grind 10 grams of MgH_2 /AlCrNiZrVNb mixtures of various ratios as indicated in Table 1. A few balls were used to stir the material during the process, which was conducted under an argon atmosphere. To reduce cold welding between particles and promote the formation of fine powder, n-heptane was used as the process control agent.

Table 1. Summary of sample composition

| Sample ID | MgH_2 (wt.%) | AlCrNiZrVNb (wt.%) |
|-----------|----------------|--------------------|
| L5 | 90 | 10 |
| L4 | 70 | 30 |
| L3 | 50 | 50 |
| L2 | 40 | 60 |
| L1 | 20 | 80 |

composition

To prevent contaminants from influencing the mechanical, interface reactivity, and physical characteristics of the milled powders, mixing was regulated under an inert gas.

Table 2. Summary of the milling parameters.

| Milling Time (hrs) | Ball (mm) | shape | Ratio (B/P) | Ball No. | Speed (rpm) |
|---------------------------|------------------|--------------|--------------------|-----------------|--------------------|
| 3 hrs | 10 | spherical | 10:1 | 100 | 200 |

The surface morphology of the unmilled and milled powders and particle size distribution were analyzed using Scanning Electron Microscopy (SEM) to gain insights into how mechanical milling affects surface texture and particle fineness. X-Ray Diffraction (XRD) was employed to determine phase composition, peak broadening, and structural deformation caused by milling, mainly indicated by the broadening and shifting of MgH_2 peaks, which suggest reduced crystallite size and increased lattice strain. Fourier Transform Infrared Spectroscopy (FTIR) was conducted to examine molecular vibrations and changes in bonds, particularly the Mg-H bonds observed in the range of $300\text{-}1700\text{ cm}^{-1}$. Together, these techniques provided a comprehensive view of the physical and chemical changes during the synthesis process. Additionally, Thermogravimetric Analysis (TGA) monitored weight loss during heating and identified thermal decomposition occurring between $400\text{ }^\circ\text{C}$ and $900\text{ }^\circ\text{C}$ at a heating rate of $10\text{ }^\circ\text{C}/\text{min}$. The effects of ball milling were studied for the first time in this research on the thermal behavior of $\text{MgH}_2/\text{AlCrNiZrVNb}$ materials intended for energy storage. The crystalline structures formed included high-entropy alloys (HEAs) and MgH_2 phases, demonstrating the material's resistance to structural degradation following ball milling. Unmilled samples exhibited sharp, well-defined peaks, whereas milled samples showed broader peaks, indicating higher lattice strain, smaller crystallite size, and grain refinement due to milling. These features are advantageous for improving hydrogen storage kinetics. Overall, the results highlight the potential of ball milling to enhance MgH_2 materials with HEA catalysts, offering improved hydrogen storage systems for energy applications.

2.2 Results

2.2.1 Microstructural analysis

2.2.1.1 SEM analysis

Figure 1 presents the SEM micrograph and corresponding EDS spectrum of MgH_2/HEA composite powders following high-energy mechanical ball milling. As shown in Figure 1(a), the particles are irregularly shaped and smaller in size, which signify the ongoing fracture and welding processes during the milling process. The surfaces of the particles are roughened due to impact and abrasion, which increases the surface area and facilitation of hydrogen diffusion. The EDS spectrum in Fig. 1(b) confirms the presence of Mg, V, Al, Cr, Nb, Zr, and Ni from HEA, and the present oxygen is a sign of oxidation on the surface that occurs during milling. Longer milling leads to better homogenization of MgH_2 and HEA particles and the development of lattice defects such as grain boundaries, strain, and dislocations, which enhance hydrogen sorption kinetics. The powders following milling are finer and

exhibit potential of partial alloying at grain surfaces. These microstructural changes play important roles in enhancing the MgH₂/HEA composites efficiency in hydrogen storage.

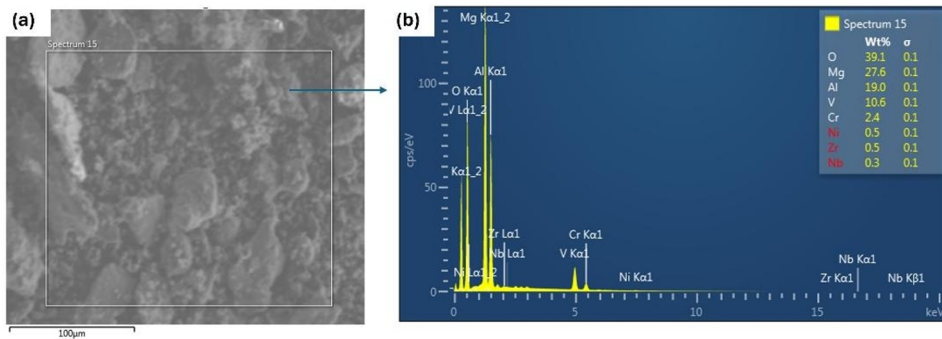


Fig. 1. (a) SEM micrograph (b) EDS of MgH₂/powders.

2.2.1.2 XRD analysis

Figure 2 presents the XRD patterns of the MgH₂/HEA composites. The powders before milling are heterogeneous and coarse, and their microstructure and properties—essential to optimize hydrogen storage performance are modified by the mechanical alloying process. XRD results show unambiguous, sharp peaks proving high crystallinity of both MgH₂ and HEA phases. The MgH₂ phase is the well-known tetragonal β-MgH₂ form, while the HEA maintains a body-centered cubic (BCC) structure, confirming the stable crystalline state of the unmilled HEA. Under unmilled situations, there was minimal contact between the two phases, as evidenced by clear and sharp peaks for HEA constituents and MgH₂. The absence of peak broadening shows relatively large grain sizes with minimal lattice strain or defect concentrations. Very ordered crystallites with minimal structural defects are evidenced by the intense peak intensities. On the other hand, the milled powders exhibit broader peaks due to increased lattice strain and smaller crystallite size caused by milling. The characteristic BCC peaks of the HEA can still be observed but can also experience minor shifts or attenuation, which are most likely the result of lattice distortion caused by milling. Due to the high crystallinity and limited contact between MgH₂ and HEA phases, poorer hydrogen sorption kinetics would be expected for the unmilled powders. Contrarily, higher hydrogen absorption and desorption kinetic activities are anticipated in milled samples owing to the larger interface area of MgH₂ and HEA phases, higher surface area, and smaller crystallite sizes. Remarkably, specimens with a higher content of MgH₂ (e.g., L5) have larger peak broadening, as would be anticipated by

higher plastic deformation of the hydride phase owing to repeated impacts during milling.

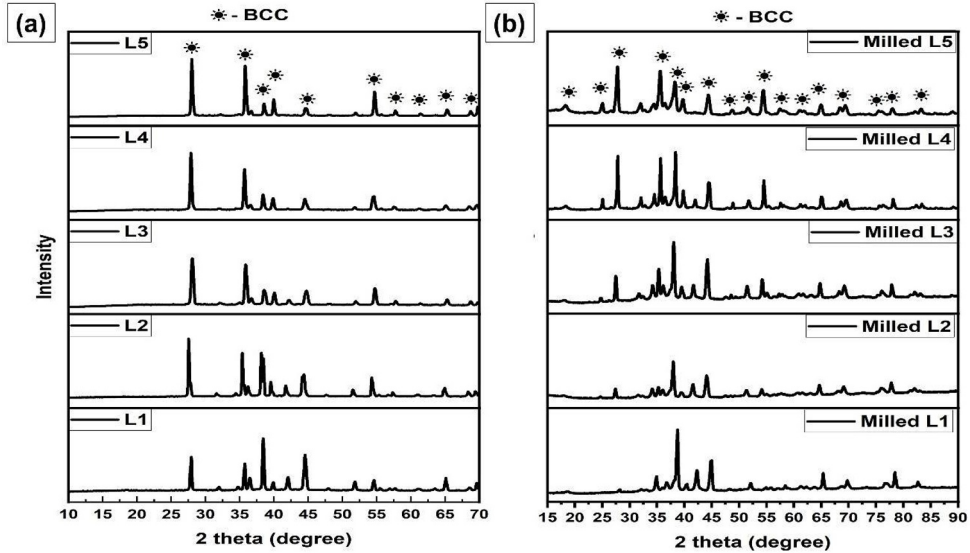


Fig. 2. XRD patterns of MgH₂/high entropy alloy powders (a) unmilled (b) milled.

2.2.2 Chemical compositional analysis

2.2.2.1 FTIR analysis

Fourier Transform Infrared (FTIR) analysis detects structural and chemical changes by monitoring variations in molecular vibrations and functional groups. Figure 3 shows FTIR spectra of MgH₂/High-Entropy Alloy powders in both unmilled and milled states. Clear and sharp peaks in the spectra indicate distinct molecular vibrations. Typical absorption bands for Mg-H bonds usually between 500 and 1000 cm⁻¹ confirm the presence of MgH₂. Bands from 1300-1700 cm⁻¹ may be linked to organic compounds. Since metallic HEAs exhibit weak IR-active modes due to their metallic bonds, their signals in the FTIR spectra are faint. Compared to the unmilled powders, the FTIR peaks of the milled samples (Figure 3b) are weaker and broader. This broadening and reduction suggest increased structural disorder and partial decomposition of the MgH₂ lattice caused by high-energy milling. Additionally, minor shifts in Mg-H peaks indicate lattice distortions in MgH₂ resulting from interactions with HEA particles during milling.

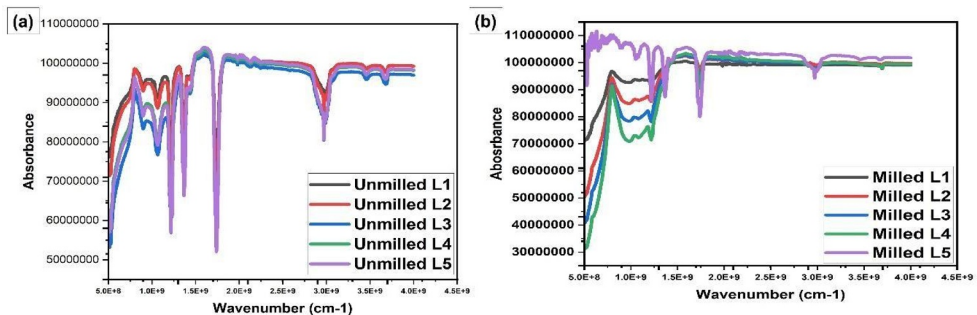


Fig. 3. FTIR curves of MgH₂/high entropy alloy powders (a) unmilled (b) milled.

2.2.3 Thermal analysis

2.2.3.1 TGA analysis

Figure 4 shows Thermogravimetric Analysis (TGA) of milled MgH_2 /High-Entropy Alloy (HEA) composites with different mass ratios labeled as L1-L5. The initial weight percentages of the samples range from about 18% for L2 to around 26% for L5, as shown on the y-axis. All samples display minimal weight loss below 400 °C, indicating good thermal stability at moderate temperatures. Significant weight loss occurs between 400 °C and 600 °C, matching the temperature range for MgH_2 decomposition into magnesium metal and hydrogen gas, with hydrogen release starting around 400 °C for most samples. Sample L5 exhibits the highest weight loss between 500 °C and 600 °C, suggesting high hydrogen desorption. Above 600 °C, some samples, like L5, show progressive weight gain due to the oxidation of magnesium and HEA components by residual oxygen in the high-temperature environment. Other samples, such as L2, display more stable weight behavior or gradual gain, indicating better oxidation resistance or thermal properties. Overall, the TGA results suggest that the HEA catalyst influences the thermal performance of MgH_2 . The samples with varying HEA content (L1 to L5) differ in hydrogen desorption efficiency and thermal stability at higher temperatures.

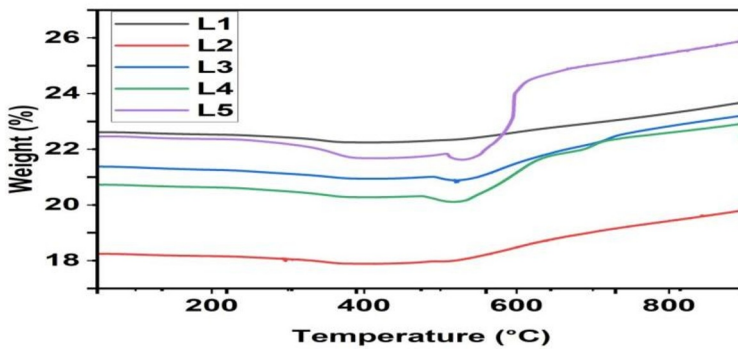


Fig. 4. TGA curves of the milled MgH_2 /high entropy alloy powders.

Milling enhances hydrogen desorption kinetics and lowers the desorption temperature by increasing the interaction between MgH_2 and HEA particles. Deviations in the TGA curves among samples L1–L5 demonstrate how different HEA concentrations influence hydrogen desorption, thermal stability, and oxidation resistance.

3 Conclusion

This study examines the effect of milling on the thermal properties and microstructure of $\text{MgH}_2/\text{AlCrNiZrVNb}$ high-entropy alloys. The results show that thermal properties favoring hydrogen absorption and desorption improve with milling. Analysis confirms that milling significantly alters the material's properties, enhancing its performance in hydrogen storage. Unmilled powders consist of segregated, coarse, highly crystalline large particles, as seen in XRD. In contrast, mechanical milling produces more refined, uniformly smaller particles with an increased surface area and closer interfaces between the MgH_2 and HEA phases, which is an essential factor since the catalytic activity of HEA depends on its proximity to MgH_2 . XRD data reveal that milling decreases crystallite size and introduces lattice strain, evidenced by peak broadening in milled samples. This structural disorder boosts hydrogen sorption kinetics. FTIR analysis supports these findings, showing prominent peaks of

absorption in the milled powders, indicating a reduced long-range structural order. Thermogravimetric analysis (TGA) indicates that the HEA catalyst influences the heat properties of MgH_2 . All samples are thermally stable with minimal weight change below 400°C ; however, between 400°C and 600°C , weight loss occurs due to MgH_2 decomposition. Differences in TGA curves among samples with varying HEA content highlight the catalyst's significant role in lowering hydrogen desorption temperature and increasing desorption rate. Overall, the results demonstrate that milling combined with the HEA catalyst effectively reduces hydrogen release temperature and enhances desorption kinetics, making this composite a promising candidate for practical hydrogen storage applications.

References

1. Al Zoubi, W., Assfour, B., Allaf, A.W., Leoni, S., Kang, J.H. and Ko, Y.G., 2023. Experimental and theoretical investigation of high-entropy-alloy/support as a catalyst for reduction reactions. *Journal of Energy Chemistry*, *81*, pp.132-142.
2. Bradbury, K. 2010. Energy Storage Technology Review.
3. Carbon Nanotubes to Nanoparticles by Ball Milling Process. *Carbon*,*37*(3), pp.493-497.
4. Couzinié, G., Dirras, L., Perrière, T., Chauveau, E., Leroy, Y., Champion, and Guillot, I., Microstructure of a near-equimolar refractory high-entropy alloy. *Materials Letters*, *285* (2014)
5. Hong, H., Guo, H., Cui, Z., Ball, A. and Nie, B., 2024. Structure modification of magnesium hydride for solid hydrogen storage. *International Journal of Hydrogen Energy*, *78*, pp.793-804.
6. Huang, S., Mechanism of magnetic transition in FeCrCoNi-based high entropy alloys. *Materials & design*, *71* (2016)
7. KONG, L.B., MA, J., ZHU, W. and TAN, O.K. 2001. Preparation of $\text{Bi}_4\text{Ti}_3\text{O}_{12}\text{Ce}$ ceramics via a High-Energy Ball Milling Process. *Materials Letters*,*51*(2), pp.108- 114.
8. Kumar, S., 2024. Comprehensive review on high entropy alloy-based coating. *Surface and Coatings Technology*, *477*, p.130327.
9. LI, Y.B., WEI, B.Q., LIANG, J., YU, Q. and WU, D.H. 1999. Transformation of
10. Liliensten, L., Couzinié, J., Perrière, L., Bourgon, J., Emery, N. and Guillot, I., New structure in refractory high-entropy alloys. *Materials Letters*, *125* (2014)
11. MHADHBI, M. 2021. Modelling of the High-Energy Ball Milling Process. *Advances in Materials Physics and Chemistry*, *11*(1), pp.31-44.
12. Nene, S.S., Sinha, S., Yadav, D.K. and Dutta, A., 2024. Metallurgical aspects of high entropy alloys. *Journal of Alloys and Compounds*, *1005*, p.175849.
13. RAMEZANI, M. and NEITZERT, T. 2012. Mechanical Milling of Aluminum Powder using Planetary Ball Milling Process. *Journal of Achievements in Materials and Manufacturing Engineering*, *55*(2), pp.790-798.
14. Rasul, M.G., Hazrat, M.A., Sattar, M.A., Jahirul, M.I. and Shearer, M.J., 2022. The future of hydrogen: Challenges on production, storage and applications. *Energy Conversion and Management*, *272*, p.116326.
15. Tokarewicz, M. and Grądzka-Dahlke, M., 2021. Review of recent research on AlCoCrFeNi high-entropy alloy. *Metals*, *11*(8), p.1302.
16. Tung, C., Yeh, J.-W., Shun, T.T., Chen, S.-K., Huang, Y.-S. and Chen, H.-C., On the elemental effect of AlCoCrCuFeNi high-entropy alloy system. *Materials letters*, *5* (2007)
17. Usman, M.R., 2022. Hydrogen storage methods: Review and current status. *Renewable and Sustainable Energy Reviews*, *167*, p.112743.

18. Wang, W. R., Wang, W. L., & Yeh, J. W. 2014. Phases, Microstructure And Mechanical Properties Of AlxCoCrFeNi High-Entropy Alloys At Elevated Temperatures. *Journal of Alloys and Compounds*, 589,
19. Wang, Y., & Zhong, W. H. 2015. Development Of Electrolytes Towards Achieving Safe And High-Performance Energy-Storage Devices: A Review. In *ChemElectroChem* (Vol. 2, Issue 1, pp. 22–36). Wiley-VCH
20. Yang, H., Ding, Z., Li, Y.T., Li, S.Y., Wu, P.K., Hou, Q.H., Zheng, Y., Gao, B., Huo, K.F., Du, W.J. and Shaw, L.L., 2023. Recent advances in kinetic and thermodynamic regulation of magnesium hydride for hydrogen storage. *Rare Metals*, 42(9), pp.2906-2927.
21. Yang, Y.F., Hu, F., Xia, T., Li, R.H., Bai, J.Y., Zhu, J.Q., Xu, J.Y. and Zhang, G.F., 2025. High entropy alloys: A review of preparation techniques, properties and industry applications. *Journal of Alloys and Compounds*, 1010, p.177691.
22. Yeh, J. W. 2006. Recent Progress In High-Entropy Alloys. *Annales de Chimie: Science Des Materiaux*, 31(6), 633–648.
23. Younas, M., Shafique, S., Hafeez, A., Javed, F. and Rehman, F., 2022. An overview of hydrogen production: current status, potential, and challenges. *Fuel*, 316, p.123317.
24. Yu, L., Zeng, K., Li, C., Lin, X., Liu, H., Shi, W., Qiu, H.J., Yuan, Y. and Yao, Y., 2022. High-entropy alloy catalysts: From bulk to nano toward highly efficient carbon and nitrogen catalysis. *Carbon Energy*, 4(5), pp.731-761.
25. Zhang, T., Uratani, J., Huang, Y., Xu, L., Griffiths, S. and Ding, Y., 2023. Hydrogen liquefaction and storage: Recent progress and perspectives. *Renewable and Sustainable Energy Reviews*, 176, p.113204.
26. Zhang, W.T., Wang, X.Q., Zhang, F.Q., Cui, X.Y., Fan, B.B., Guo, J.M., Guo, Z.M., Huang, R., Huang, W., Li, X.B. and Li, M.R., 2024. Frontiers in high entropy alloys and high entropy functional materials. *Rare Metals*, 43(10), pp.4639-4776.